

Spin-glass-like magnetic properties for $R\text{Fe}_{10}\text{Mo}_2$ compounds ($R = \text{Y}$ or Lu) with the ThMn_{12} -type structure

C. Christides, A. Kostikas, G. Zouganelis, and V. Psyharis

*Institute of Materials Science, National Center for Scientific Research (NCSR) "DEMOKRITOS,"
153 10 Aghia Paraskevi Attiki, Greece*

X. C. Kou and R. Grossinger

Institut für Experimentalphysik, Techn. Univ. Vienna, A-1040 Vienna, Austria

(Received 28 September 1992)

dc and ac magnetic measurements combined with Mössbauer spectroscopy have been used to study the evolution of magnetic order below the critical temperature T_c in polycrystalline powders of the intermetallic compounds $\text{YFe}_{10}\text{Mo}_2$ and $\text{LuFe}_{10}\text{Mo}_2$. Irreversibility of the dc thermomagnetic curves after zero-field-cooling (ZFC) and field-cooling (FC) processes has been observed. A hysteresis loop has been detected for both compounds at 4.5 K and a shifting of the loop after FC has been observed in $\text{LuFe}_{10}\text{Mo}_2$. Strong spin-relaxation effects were recorded in ^{57}Fe Mössbauer absorption spectra in temperatures well below the $T_c = 360$ and 260 K for $R = \text{Y}$ and Lu alloys, respectively. Furthermore, a number of magnetic properties common to conventional spin glasses and true ferromagnets has been revealed, which suggest the existence of a spin-glass-like magnetic phase below T_c .

INTRODUCTION

The nature of the magnetic-moment configurations known under the generic name of spin glasses and the conditions required for their attainment have been the subject of a great number of experimental and theoretical investigations during the past several years.¹ Although the prototype spin-glass behavior has been observed and studied initially in crystalline dilute alloys of magnetic $3d$ elements in noble metals, a large amount of data now exists demonstrating the appearance of properties which are considered characteristic of a spin-glass state in iron-rich amorphous alloys, where the structural disorder creates the conditions of a distribution of competing exchange interactions which are presumably required for the establishment of a spin-glass state. Experimentally, spin-glass behavior is usually identified by the observation of a few typical features—a cusp in the temperature dependence of the ac susceptibility, irreversible behavior of magnetization versus temperature below the freezing temperature, appearance of coercivity in the spin glass state—but the nature of the magnetic state is still a matter of considerable controversy. It may be argued, indeed, that the observation of similarities in different systems does not necessarily imply identical magnetic structures. In recent years several studies have been concerned with the so-called "reentrant" type of magnetic systems which are close to the limit of ferromagnetic order and exhibit a transition from ferromagnetic to noncollinear order with decreasing temperature. A typical, well-studied example of an iron-rich system of this type is the class of amorphous $\text{Fe}_x\text{Zr}_{1-x}$ alloys at values of $0.93 > x > 0.88$.² A second magnetic transition is observed well below T_c by several techniques including dc and ac susceptibilities,^{3,4} small-angle neutron scattering (SANS) (Ref. 5) and Mössbauer spectroscopy.^{2,6} Similar results have been obtained with a series of amorphous

yttrium-iron alloys of the general formula $\text{Y}_{1-x}\text{Fe}_x$ with $0.32 > x > 0.88$ by Coey *et al.*⁷ The data from these investigations have been rationalized with a model that assumes a distribution of Fe-Fe exchange interactions with positive average value J and a width Δ extending to negative values. On the basis of the mean-field mixed exchange theory of Gabay and Toulouse,⁸ a phase diagram in the plane $(T, J/\Delta)$ has been proposed by Ryan *et al.*² which outlines the region between the conventional spin glass and ferromagnetic behavior. At temperatures below the paramagnetic regime, as J/Δ is reduced from high values ($J/\Delta \geq 3$) where the spin system shows conventional ferromagnetic behavior with infinite correlation length, a region of collinear order sets in with a locally preferred axis whose direction is maintained over a finite coherence length of 20–30 nm. The average magnetic moment is zero but a small magnetic field can produce significant alignment of the local axes although the magnetization remains below saturation because of the presence of rapidly rotating perpendicular components. At these values of J/Δ as the temperature is lowered the perpendicular spin components freeze leading to an anisotropic distribution of orientation of the magnetic moments, which has been termed an asperomagnetic configuration.¹ Evidence for the gradual passage from ferromagnetic to noncollinear order has been found in studies of hydrogenated amorphous Y-Fe alloys where J/Δ can be varied by changing the hydrogen concentration.⁹

We report in this communication the observation of similar spin-glass-like phenomena in the crystalline ternary alloys $\text{YFe}_{10}\text{Mo}_2$ and $\text{LuFe}_{10}\text{Mo}_2$. These alloys are members of a class of compounds crystallizing in the ThMn_{12} type of structure with the general formula $R\text{Fe}_{10-x}\text{T}_x$ ($2 \geq x > 1$), with R a rare-earth metal and $T = \text{Ti, V, Cr, W, Si, Mo}$. They have been studied extensively in recent years as candidates for permanent magnet ma-

terials.^{10–12} The Mo members of this series with $x = 2$ are exceptional in their intrinsic magnetic properties in several respects. A variety of magnetic phase transitions (MPT) has been observed with descending temperature and for the compounds with heavy rare earths very unusual magnetic properties appear for different R .^{13,14} A detailed description of these results will be presented in a forthcoming paper. We mention only some of the features of the magnetic properties of these alloys which set them apart from the other groups and presage the appearance of uncommon types of magnetic configurations: (a) The values of the Curie temperatures (T_c) and saturation magnetization (M_s) are nearly 30% and 20% lower, respectively, relative to the other $R(\text{Fe},\text{M})_{12}$ studied series of 1:12 compounds with $M = \text{Ti}, \text{V}, \text{Cr}, \text{W},$ and Si . Since the lattice constants of the Mo series are not significantly different from the other series, the difference in T_c and M_s indicates a strong modification of the $3d$ bands due to the contribution of the extra d states from Mo in the $3d$ band of the Fe host.¹⁵ (b) A considerable decrease ($\sim 50\%$) of the ordering temperature T_c is observed from $R = \text{Gd}$ to Lu alloys which is accompanied by the observation of strong relaxation effects in the ^{57}Fe Mössbauer absorption spectra. (c) From singular point detection (SPD) results on $\text{YFe}_{10}\text{Mo}_2$ and $\text{GdFe}_{10}\text{Mo}_2$ it is concluded that the Fe sublattice possesses uniaxial anisotropy. In view of this, the appearance of a MPT in the compounds with the nonmagnetic Y and Lu, clearly evident in the ac susceptibility data,¹⁴ is unexpected. We present in this paper detailed results which suggest that the magnetic state has many of the features of a spin-glass configuration.

The observation of spin-glass-like phenomena in compounds with the 1:12 type of structure has been reported several years ago in a detailed magnetization and Mössbauer study of the alloys $\text{YFe}_x\text{Al}_{12-x}$.¹⁶ In this study it has been demonstrated that as the Fe concentration increases from $x = 4$ to $x = 6$ the distribution of Fe in the three crystallographic sites f , i , and j of the 1:12 lattice changes, respectively, from an almost unique occupation of the f site giving rise to an antiferromagnetic state, to a preferential occupation of the i and j sites. This leads to the randomness of exchange interactions required for the occurrence of a spin-glass state. More recently evidence has also been presented from neutron diffraction and magnetization measurements that a spin-glass transition occurs in HoFe_4Al_8 .¹⁷ In our work the alloys studied are much richer in Fe, but apparently the randomness of exchange interactions persists, leading to a noncollinear magnetic state similar to that observed in the iron-rich amorphous alloys mentioned above.

In the following sections we shall first present the experimental results which support the establishment of a noncollinear type of magnetic order and then discuss these results in the light of theoretical models leading to this state.

EXPERIMENTAL RESULTS

A. Preparation and structural characterization

The samples of the alloys were prepared by arc melting from 99.99% starting materials. The as-prepared ingots

were vacuum annealed at 850°C for 5 days. From x-ray powder patterns obtained with a Siemens D500 diffractometer the samples were found to be single phase with the tetragonal ThMn_{12} type structure. It is worth noting that the several heat treatments and annealing times performed on three separately prepared ingots for each alloy with $R = \text{Y}, \text{La}$ do not show any difference from the vacuum-annealed samples at 850°C for 5 days. We consider therefore that within the resolution of our measurements the observed phenomena are not caused by homogenization effects of the ingots. The lattice constants and the atomic positions were determined by Rietveld analysis of the x-ray diffractograms and are listed in Table I for the two studied compounds. In this analysis the Mo was assumed to substitute for two iron atoms in the i site of the unit cell in accordance with a previous detailed study of $\text{SmFe}_{10}\text{Mo}_2$ and its nitride.¹⁸ In the same table we have also listed the interatomic Fe-Fe distances calculated with the results of the structure analysis.

B. Magnetic measurements

Magnetic dc measurements were obtained with a vibrating sample magnetometer up to applied fields of 2 T. The temperature dependence of the saturation magnetization for both alloys measured in a field of 2 T is shown in Fig. 1. The saturation moments at 4.5 K are $12.8\mu_B$ and $10.6\mu_B$ per formula unit for the Y and Lu alloys, respectively. Thermomagnetic dc measurements were also performed at lower applied fields, with zero field cooling (ZFC) and field cooling (FC) procedures. The thermal variation of magnetization in two different applied homogeneous fields is plotted in Fig. 2 for $R = \text{Y}$. The data for an applied field of 50 mT show that for the field-cooled procedure the temperature dependence is the same when measured with increasing or decreasing temperature. The difference between the ZFC and FC curves indicates the appearance of irreversibility at a temperature of about 260 K for this field. Furthermore, from measurements at a higher field it is found that a coincidence of the thermomagnetic curves from the ZFC or FC procedures occurs for an applied field of approximately 0.7 T. On the other hand, the persistence of the irreversible behavior for very low-dc applied fields (2 mT), shown in Fig. 2(b), excludes the appearance of this effect because of the magnetic domain structure of the material. From the data of Fig. 2(a) the Curie temperature of the Y alloy is estimated at 350 K, in agreement with the previously reported value.¹⁹ It is interesting to note that for the Lu compound substantial magnetization can be induced even by small fields, making it difficult to estimate the Curie temperature. An approximate value of 260 K can be assumed on the basis of the Mössbauer data which show only a paramagnetic component above this temperature (see below).

The nature of irreversibility in the thermomagnetic measurements has been investigated in more detail for the Lu alloy by a series of thermomagnetic cycles following a similar procedure to that used by Wakabayashi *et al.* in a study of amorphous Fe-La alloys.²⁰ This procedure is aimed at exploring the relation between irrever-

TABLE I. Lattice constants, fractional atomic coordinates, and neighbor distances smaller than 3.5 Å for $\text{YFe}_{10}\text{Mo}_2$ and $\text{LuFe}_{10}\text{Mo}_2$.

$\text{YFe}_{10}\text{Mo}_2$				$\text{LuFe}_{10}\text{Mo}_2$			
a (Å)	b (Å)	c (Å)		a (Å)	b (Å)	c (Å)	
8.544	8.544	4.792		8.511	8.511	4.780	
Atom	Site	x	y	z	x	y	z
$R = \text{Y, Lu}$	a	0.000	0.000	0.000	0.000	0.000	0.000
Fe-Mo	i	0.359	0.000	0.000	0.356	0.000	0.000
Fe	j	0.275	0.500	0.000	0.278	0.500	0.000
Fe	f	0.250	0.250	0.250	0.250	0.250	0.250

Site	Neighbor	Number	Distance (Å)	
			$\text{YFe}_{10}\text{Mo}_2$	$\text{LuFe}_{10}\text{Mo}_2$
i	i	1	2.402	2.433
	i	4	2.933	2.944
	j	2	2.633	2.653
	j	2	2.651	2.663
	f	4	2.609	2.602
	a	2	3.052	3.033
j	i	2	2.633	2.653
	i	2	2.651	2.663
	j	2	2.702	2.660
	f	4	2.449	2.450
	a	2	3.061	3.041
f	i	4	2.609	2.602
	j	4	2.449	2.450
	f	4	2.392	2.389
	a	2	3.237	3.234

sibility and the model of a free energy surface with a large number of minima corresponding to quasiequilibrium states which has been proposed by theoretical considerations.²¹ The experimental results are summarized in Fig. 3 where the numbers refer to the sequence of temperature and applied field changes. Initially, the temperature dependence of the magnetization was measured by cooling from 200 to 4.5 K in a field of 20 mT and then warming up again to 200 K. This procedure is reversible.

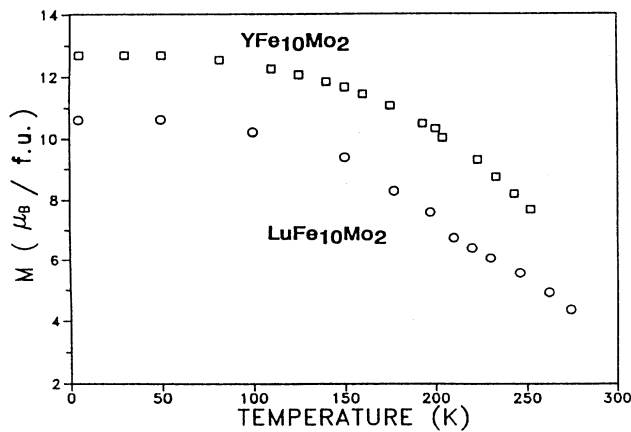


FIG. 1. Temperature dependence of the saturation magnetization of $\text{YFe}_{10}\text{Mo}_2$ and $\text{LuFe}_{10}\text{Mo}_2$.

After this measurement the following thermomagnetic protocol was executed.

(1) Starting with a zero-field-cooled (ZFC) state from above 200 to 4.5 K a field of 20 mT is applied (point 1) and the magnetization in this field with increasing temperature is measured up to 200 K.

(2) At $T = 200$ K the field is lowered to 6 mT (point 3). This step is reversible.

(3) Cooling in a field of 6 mT to 4.5 K and increasing the field to 20 mT (sequence 3-4-5) leads to a state different from that of the ZFC sample in 20 mT (point 1). The temperature dependence now to 200 K follows a different curve to point 6.

(4) Following the same route as before (points 6-7-8-9) we arrive at the same state as point 5. Increasing the temperature to 110 K the magnetization follows the same path up to point 10.

(5) By field cooling back to 4.5 K we obtain the state at point 11. The return to 10 is reversible.

(6) The following cycle (10-12-13-14-10) is obtained by lowering the field to 10 mT, then the temperature to 4.5 K and restoring the field to 20 mT. Increasing the temperature in this field leads back to point 10.

(7) Finally, the field is increased to 26 mT leading to point 15. Subsequent cooling under this field leads to state 16 and return to a field of 20 mT gives state 17. Heating to 110 K gives a state which is different from the initial state 10 at the same temperature and field. By increasing the temperature further to 200 K the same state

is obtained as in previous cycles.

The main feature emerging from the preceding observations is that the magnetization as a parameter describing the state of the system is not a unique function of B and T below 200 K. In other words, the value of the magnetization at a given B and T depends on previous history with regard to temperature and field changes. This is exemplified by points 1, 5, 9, 14, and 17 which correspond to the same values of B and T (20 mT and 4.5 K, respectively) but exhibit different magnetic moments. In the picture of the free energy surface this means that the system is in different local minima. Furthermore we observe that processes which involve lowering of the field and/or the temperature (e.g., 10-11-10 or 10-12-13-14) do not change the minimum at which the system resides, while increasing the field at constant temperature causes a change in local minimum (procedure 10-15-16-17). These results are typical of quasiequilibrium states of a spin-glass system.²¹

The nature of the magnetic state below the temperature at which irreversibility sets in, has been also examined by thermoremanence (TRM) and isothermal

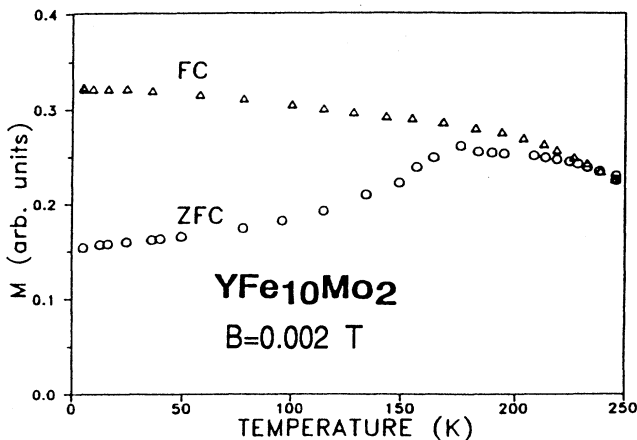
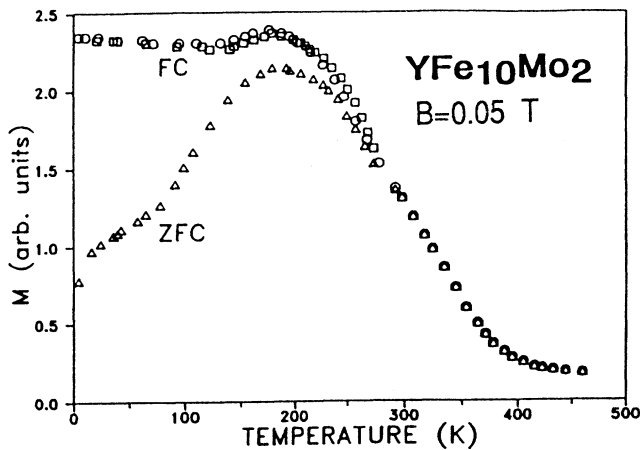


FIG. 2. Temperature dependence of the magnetization of $\text{YFe}_{10}\text{Mo}_2$ for ZFC and FC samples at two values of the applied field.

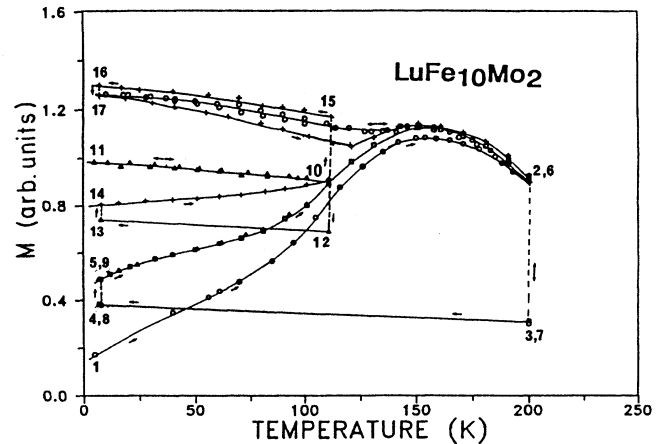


FIG. 3. Thermomagnetic cycles performed on $\text{LuFe}_{10}\text{Mo}_2$. For a detailed explanation see text.

remanence (IRM) measurements. TRM and IRM data were obtained for the Y alloy at $T=4.5$ K up to a maximum applied field of 2 T. The results are shown in Fig. 4. The thermoremanence was measured by cooling the sample from a temperature $T > 250$ K to 4.5 K in a magnetic field B and measuring the magnetic moment after removing the field. The isothermal remanence was measured by applying a field B on a ZFC sample at 4.5 K and then removing the field. Time relaxation effects have been observed for each measurement of the remanence magnetization and the points in Fig. 4 represent values observed after 5 s from the removal of the applied field. Every point has been measured after a cycle of heating-up to 250 K and cooling down to 4.5 K. We note that the TRM and IRM curves do not meet up to the highest field of 2 T used in these measurements.

Evidence for the occurrence of magnetic phase transitions well below the estimated Curie temperatures is given by ac susceptibility measurements as reported already earlier.¹⁴ Plots of the real part of the ac suscepti-

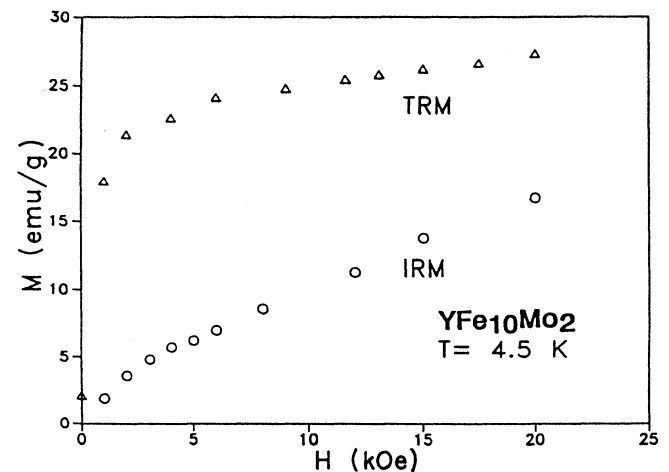


FIG. 4. Thermoremanence (TRM) and isothermal remanence (IRM) results for $\text{YFe}_{10}\text{Mo}_2$.

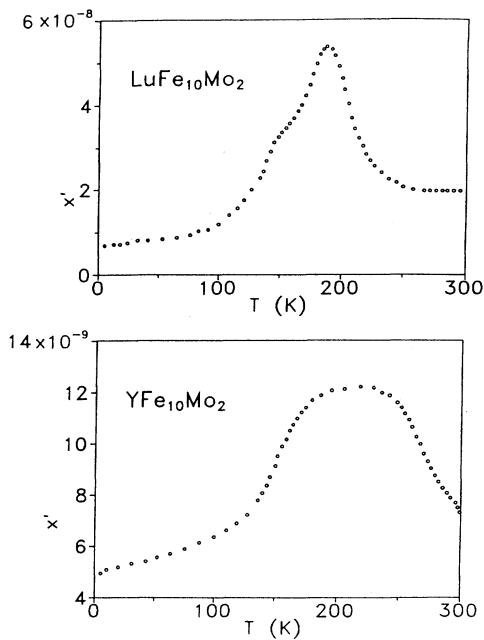


FIG. 5. Temperature dependence of the real part of the ac susceptibility of $\text{YFe}_{10}\text{Mo}_2$ and $\text{LuFe}_{10}\text{Mo}_2$.

bility as a function of temperature are shown in Fig. 5. The Y alloy data show a rise to a plateau below 300 K and then a sharp drop at approximately 150 K. The Lu alloy exhibits a peak at 180 K which is close to the temperature at which irreversibility sets in the dc magnetization data. A shoulder is also observed in the Lu alloy data which may indicate the occurrence of a second magnetic phase transition. Since Y and Lu are nonmagnetic, the MPT must be associated with the Fe sublattices. Magnetic anisotropy data obtained with the singular point detection (SPD) technique show axial anisotropy over the entire temperature range. The results for the Y alloy are shown in Fig. 6 where also the corresponding results for $\text{GdFe}_{10}\text{Mo}_2$ are plotted for comparison. The curve for the Y alloy shows a discontinuity in slope at about 150 K, the same temperature at which the sharp drop in ac susceptibility is observed. In contrast the Gd alloy shows a smooth monotonic decrease of the anisotropy

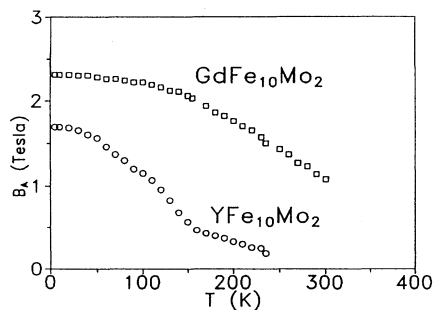


FIG. 6. Temperature dependence of the anisotropy field for $\text{GdFe}_{10}\text{Mo}_2$ and $\text{YFe}_{10}\text{Mo}_2$ measured by the SPD technique.

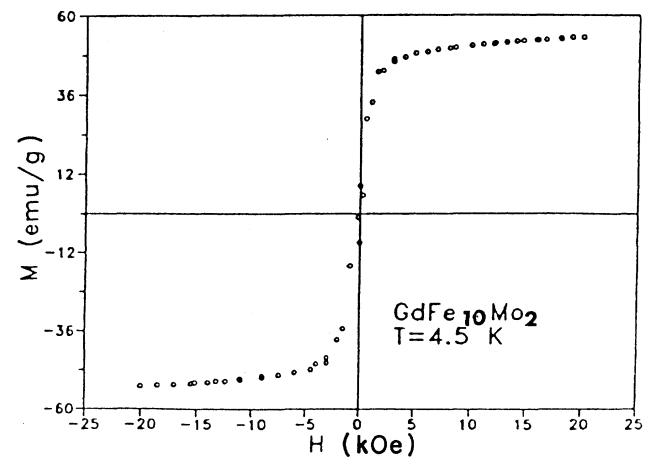
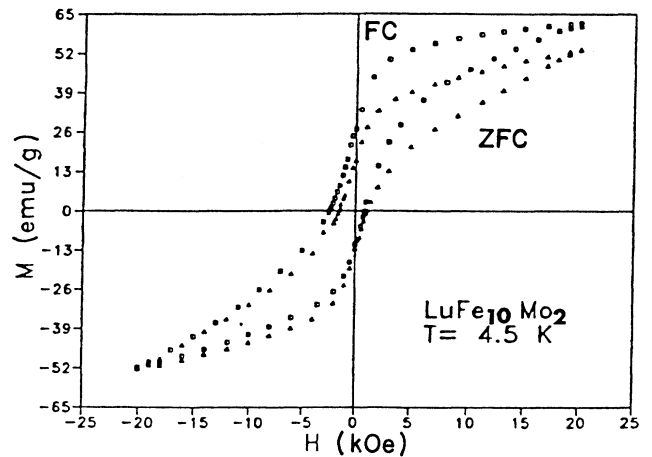
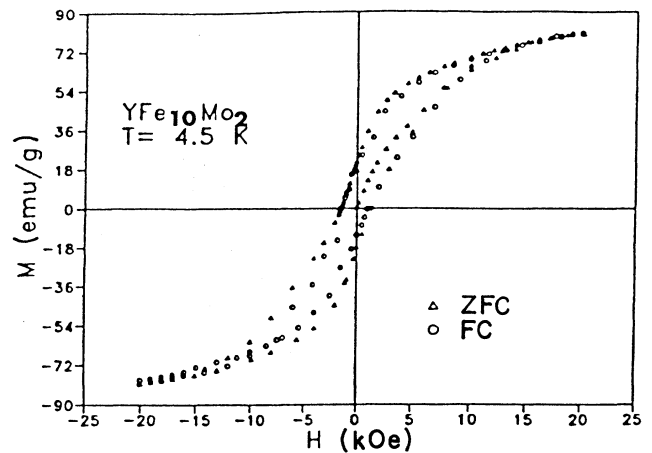


FIG. 7. Hysteresis loops for ZFC and FC samples of $\text{YFe}_{10}\text{Mo}_2$, $\text{LuFe}_{10}\text{Mo}_2$. The $\text{GdFe}_{10}\text{Mo}_2$ loop is also given for comparison.

py field with increasing temperature. Hysteresis loops were measured at 4.5 K on FC and ZFC samples of both alloys. For comparison a hysteresis loop was also measured for the Gd alloy in this series. The results are shown in Fig. 7. The Y and Lu alloys show coercivities in the range of 0.2 to 0.3 T while for the Gd alloy the coercivity is practically zero. The maximum anisotropy field observed for the Y alloy at 4.5 K measured by the SPD technique, is lower than that obtained in $\text{GdFe}_{10}\text{Mo}_2$ (Fig. 6) and since in both cases the anisotropy field is caused in a first approximation from the Fe sublattice, the absence of a hysteresis loop in the temperature range from 4.5 K up to $T_c = 440$ K for $R = \text{Gd}$ is a strong evidence that the observed loop for $R = \text{Y, Lu}$ is induced from some intrinsic properties of this material correlated to a special magnetic configuration of the system. A symmetric narrowing of the loops around the origin of the axis is observed by decreasing the maximum field B_{max} which is closing the loop. The variation of the observed coercive field for the Y alloy at 4.5 K as a function of B_{max} , shown in Fig. 8(a), is indicative that the ob-

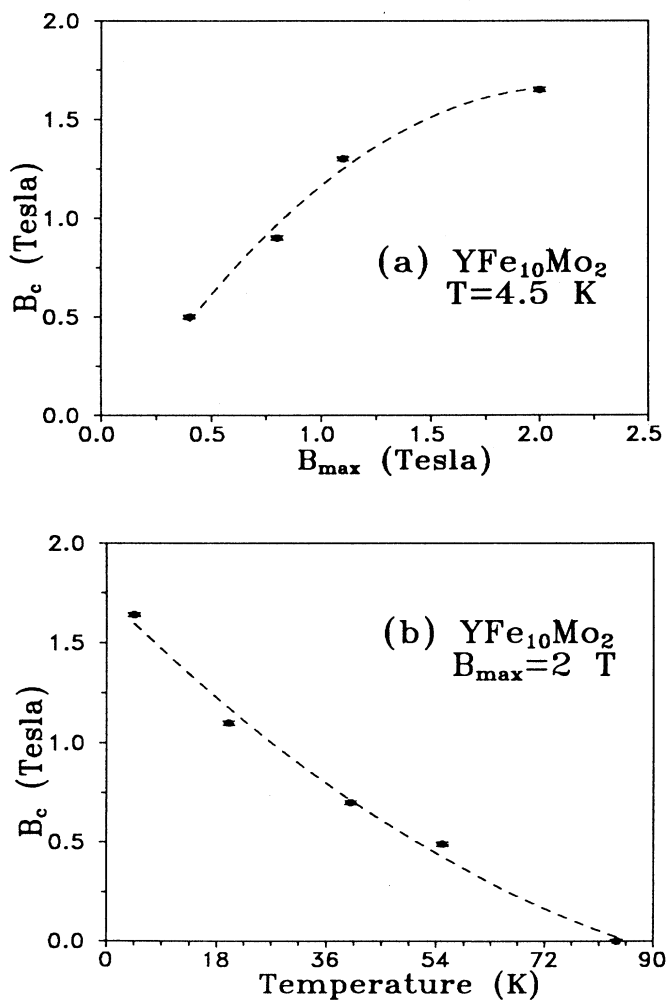


FIG. 8. The dependence of the coercive field of $\text{YFe}_{10}\text{Mo}_2$ on (a) the maximum applied field and (b) the temperature.

served loop for $B_{\text{max}} = 2$ T (Fig. 7) is close to the saturation of B_c . The temperature dependence of B_c in Fig. 8(b) shows that the hysteresis loop vanishes at 84 K which is well below 150 K where the B_A vs T curve changes slope (Fig. 6). On the other hand the hysteresis loop for the field-cooled sample of the Lu alloy is displaced asymmetrically, a feature that has been found in studies of spin glasses.²²

C. ^{57}Fe Mössbauer spectra

Mössbauer measurements were obtained in the temperature range of 5–300 K using a conventional constant acceleration spectrometer with a $^{57}\text{Co}(\text{Rh})$ source. The results for the Y and Lu alloys are shown in Figs. 9 and 10, respectively. The main feature of the absorption spectra for both alloys is the appearance of considerable paramagnetic components well below the estimated values of the Curie temperatures. For the Lu alloy, for

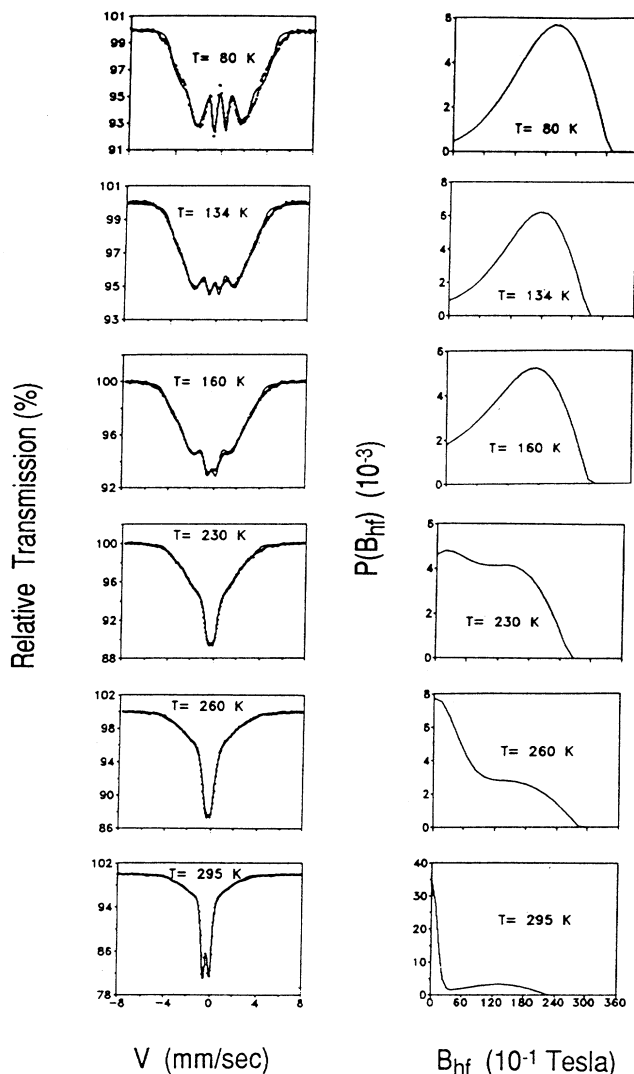


FIG. 9. Mössbauer spectra and hyperfine field distributions of $\text{YFe}_{10}\text{Mo}_2$ at different temperatures.

example, the spectrum is completely paramagnetic at 250 K while the magnetization data indicate that substantial magnetization can be induced even at small fields. Moreover, the magnetic hyperfine components show broad unresolved lines, similar to those observed in amorphous alloys implying a distribution of hyperfine fields. To account for these features the spectra have been simulated with a bimodal distribution of hyperfine fields, similar to that used for the analysis of Fe-Ni alloys,²³ including a "ferromagnetic" and a "paramagnetic" component with fractional occupations f_x and $1-f_x$, respectively. For the "ferromagnetic" component we have used a modified Gaussian distribution with a maximum at B_0 and a cut-off at $B = B_0 + B'$:

$$F_f(B) = f_x(B_0 + B' - B)B'^{-2} \\ \times \exp[-(B - B_0 - B')^2/2B'^2]$$

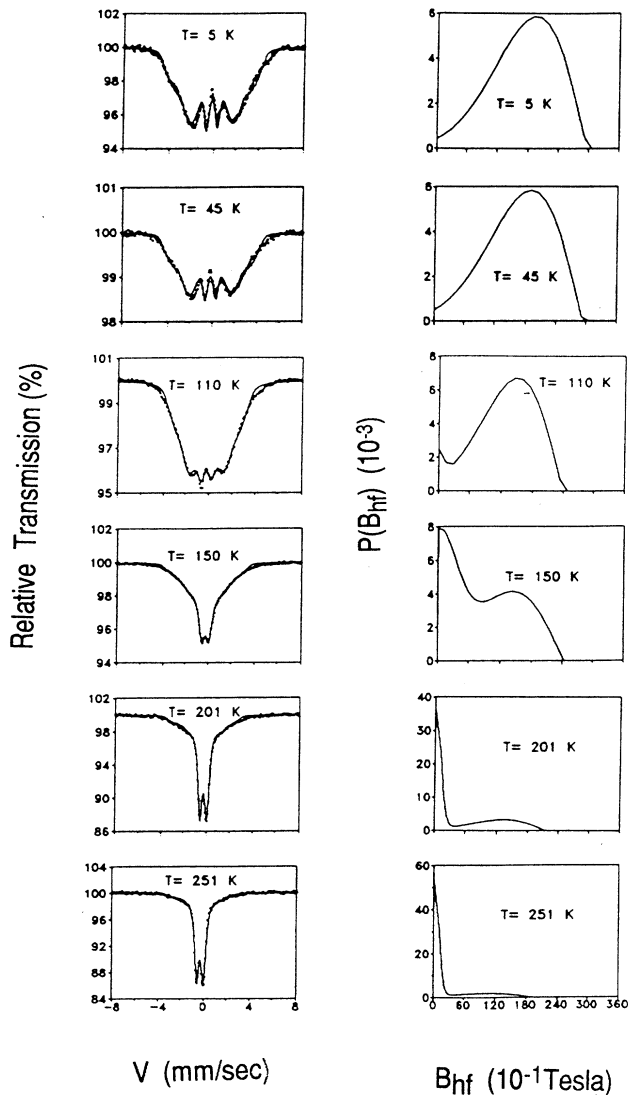


FIG. 10. Mössbauer spectra and hyperfine field distributions of $\text{LuFe}_{10}\text{Mo}_2$ at different temperatures.

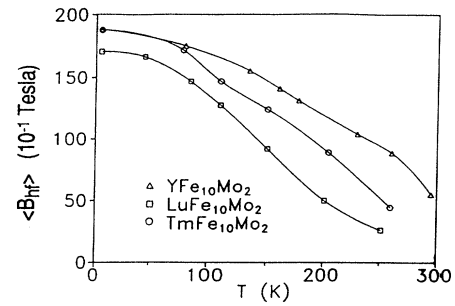


FIG. 11. Temperature dependence of the average hyperfine field for $\text{YFe}_{10}\text{Mo}_2$ and $\text{LuFe}_{10}\text{Mo}_2$. The temperature dependence of $\text{TmFe}_{10}\text{Mo}_2$ is also shown for comparison.

for $0 < B < B_0 + B'$. For the paramagnetic component the probability distribution was taken as a simple Gaussian:

$$F_p(B) = (1 - f_x)(2/\Gamma_p\pi^{1/2})\exp(-B^2/\Gamma_p^2)$$

for $B \geq 0$. The hyperfine field distributions derived from this procedure are shown also in Figs. 9 and 10. The average magnetic hyperfine fields $\langle B_{\text{hf}} \rangle$ as a function of temperature are plotted in Fig. 11 and the estimated percentage of the ferromagnetic component f_x is given in Fig. 12. For comparison we have included also in these figures the results for $\text{TmFe}_{10}\text{Mo}_2$ which shows intermediate behavior.

The variation of the average hyperfine fields presents an inflection for $R = \text{Lu}$ at temperatures near 200 K. This anomaly is more evident in the variation of f_x suggesting that in $\text{LuFe}_{10}\text{Mo}_2$ significant freezing of spin components appears below 200 K. On the other hand, the persistence of a paramagnetic component down to 150 K indicates the existence of clusters with rapidly fluctuating spins which order gradually as the temperature decreases. We shall discuss these effects in greater detail in the next section in connection with the magnetization results.

DISCUSSION

The experimental results presented in the preceding section contain several features which suggest that the or-

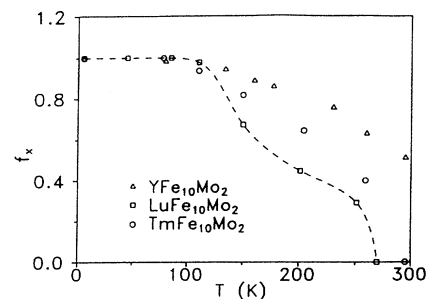


FIG. 12. Temperature dependence of the magnetic fraction for $\text{YFe}_{10}\text{Mo}_2$ and $\text{LuFe}_{10}\text{Mo}_2$. The temperature dependence of $\text{TmFe}_{10}\text{Mo}_2$ is also shown for comparison.

dering in the $\text{LuFe}_{10}\text{Mo}_2$ and $\text{YFe}_{10}\text{Mo}_2$ alloys is established by spin freezing in a noncollinear magnetic configuration. The qualitative aspects of these results are summarized in Table II. In many ways the observed behavior is similar to that observed in iron-rich amorphous Y-Fe alloys.⁷

The appearance of irreversibility and hysteresis, manifested by the difference in measurements of ZFC and FC samples and the IRM and TRM values is the strongest evidence for the establishment of a spin-glass-like state. These phenomena appear at temperatures well below the estimated ferromagnetic ordering temperatures and cannot be explained as arising from some special type of magnetic domain configuration for two reasons: (a) the difference in the temperature dependence of the magnetization in FC and ZFC samples persists at low fields and (b) the homologous Gd alloy shows in all respects normal ferrimagnetic behavior with no irreversibility or hysteresis.

Theoretical models of spin-glass systems with the observed properties are generally based on a distribution of exchange interactions with positive average value J and width Δ , extending to negative values of the exchange interaction.^{8,21} In amorphous alloys the distribution arises from the distribution of interatomic distances and the variation of the number of nearest neighbors. In the crystalline systems studied in this paper, the distribution can be attributed to the variation of Fe-Fe distances in different lattice sites and the distribution of Mo atoms in the unit cell. The structure results given in Table I reveal significant differences in interatomic Fe-Fe distances extending from 2.389 to 2.944 Å. At the lower end of this range the Fe-Fe interactions are expected to be negative. The transition from ferromagnetic to antiferromagnetic

interaction in direct exchange between $3d$ orbitals is estimated from the well-known Slater-Néel curve to occur to approximately 2.5 Å.²⁴ This estimate is supported by experimental studies of fcc iron both in thin film form²⁵ and as a precipitate in copper.²⁶ The existence of negative exchange interactions has also been established in the crystalline $\text{Lu}_2\text{Fe}_{17}$ alloy where certain pairs of Fe atoms occur with distances smaller than 2.5 Å.²⁷ In this case the competition between positive and negative interactions leads to a helimagnetic structure. In the ThMn_{12} structure of the studied alloys, from the data of Table I, it is seen that distances below 2.5 Å occur for several pairs of Fe atoms, with the lowest distance of 2.392 Å observed for the Fe(f)-Fe(f) pair. This observation explains the antiferromagnetic order found in the YFe_4Al_8 alloy¹⁶ where Fe occupies exclusively the f site. When the Fe concentration increases the iron atoms are randomly distributed in the three crystallographic sites and pronounced spin-glass phenomena are observed in the YFe_5Al_7 alloy. This alloy exhibits hysteresis loops and a temperature dependence of the coercive field similar to our results. Finally, additional evidence that the observed magnetic behavior is due to a specific distribution of magnetic exchange interactions is offered by the change in magnetic properties induced by nitrogenation of these alloys.²⁸ The introduction of nitrogen increases dramatically the Curie temperature, e.g., from 350 to 520 K for the Y alloy and from about 260 to 470 K for the Lu alloy. Moreover, although high-anisotropy fields are observed, no significant hysteresis appears. It may therefore be suggested that the effect of nitrogen is to shift the distribution of exchange interactions to more positive values in the ferromagnetic regime of the phase diagram proposed by Ryan *et al.*² This effect is similar to the observed shift of the magnetic behavior of amorphous Y-Fe alloys upon hydrogenation.⁹

Although the major source for the uncommon magnetic properties of the studied alloys can be attributed to competing positive and negative exchange interactions, a significant role may also be played by electronic effects as expressed in the electronic band structure. This can be surmised from the difference in Curie temperatures of the compounds $\text{YFe}_{10}\text{Cr}_2$ and $\text{YFe}_{10}\text{Mo}_2$ (510 and 350 K, respectively) which have the same number of valence electrons. The effect can be understood qualitatively from the difference of the perturbation of the $3d$ bands of Fe by the introduction of Cr and Mo.¹⁶ It must be noted also that our results show that although there is little difference in interatomic distances between the Y and Lu compounds, the former is closer to the ferromagnetic regime than the latter. XPS measurements may shed more light to this question.

As already mentioned, the Mössbauer spectra also provide evidence for freezing of spin components at temperatures below the estimated Curie temperature. This is shown by the inflection point in the temperature dependence of the average hyperfine field (Fig. 10), which is clear mainly in the Lu alloy data. Another expected characteristic of transverse spin freezing is the development of a discrepancy between moments determined by Mössbauer spectroscopy and M_s deduced from iso-

TABLE II. Magnetic properties observed in $\text{YFe}_{10}\text{Mo}_2$ and $\text{LuFe}_{10}\text{Mo}_2$ alloys, indicative of the existence of a spin-glass-like magnetic ordering below the T_c .

Magnetic property	$\text{YFe}_{10}\text{Mo}_2$	$\text{LuFe}_{10}\text{Mo}_2$
1. Irreversibility of dc M vs T curve from ZFC and FC process	Yes	Yes
2. ac-susceptibility x' and x'' vs T transitions	Yes	Yes
3. Hysteresis loop at low T	Yes	Yes
4. Shift of the hysteresis loop after ZFC and FC	No	Yes
5. Difference of TRM and IRM curves measured at 4.5 K	Yes	NA
6. Slope change of B_A vs T curve measured from the SPD method	Yes	NA
7. Strong relaxation effects of Mössbauer spectra for $T > 100$ K	Yes	Yes
8. Difference between M_s and $\langle H_{\text{hf}} \rangle$ magnetic moments at 5 K	No	Yes
9. Slope change of $\langle H_{\text{hf}} \rangle$ T curve by lowering T	No	Yes

thermal magnetization curves. This arises because between T_c and the temperature of freezing of transverse components T_{xy} only the z components of the spins are ordered and both techniques observe the same moment. Below T_{xy} the total moment increases and Mössbauer spectra measure this, but the maximum magnetic field applied for magnetization measurements usually is not enough to align the noncollinear moments and the observed M_s should always be less than that obtained from the average hyperfine splitting. Using a conversion factor of $14.6\mu_B/T$ we have found an average magnetic moment of $13\mu_B/f.u.$ from the $\langle B_{hf} \rangle = 19$ T at 4.5 K for $R=Y$, in accordance to M_s obtained from magnetization measurements. In the case of $\text{LuFe}_{10}\text{Mo}_2$ the $\langle B_{hf} \rangle = 17.5$ T gives $12\mu_B/f.u.$ which is considerably larger than $10.6\mu_B/f.u.$ obtained from isothermal magnetic measurements at 4.5 K. This is an additional indication that the Lu alloy has clearly more properties of a noncollinear configuration of magnetic moments while the Y alloy is closer to the ferromagnetic regime. A measurement of magnetic spectra in a high-applied magnetic field could give a definitive result on the noncollinear nature of the magnetic state.

The Mössbauer results provide also qualitative information about the dynamics of the establishment of magnetic order. It has been noted that a considerable paramagnetic component persists at temperatures well below the estimated Curie temperature. This infers that a substantial fraction of ^{57}Fe nuclei is sensing an effective field which fluctuates rapidly within the nuclear lifetime. Similar line shapes have been observed in the cluster glass $\text{Y}_{1.1}(\text{Fe}_{0.75}\text{Al}_{0.25})_2$ and have been simulated with a relaxation model which assumes that magnetic clusters form stochastically and decay after a mean lifetime which increases with increasing applied field and decreasing temperature.²⁹

On the basis of the experimental results and the above discussion we may propose the following tentative model for the evolution of magnetic order in the $\text{YFe}_{10}\text{Mo}_2$ and $\text{LuFe}_{10}\text{Mo}_2$ alloys: As the temperature decreases from the paramagnetic regime short-range spin correlations are established in a direction determined by the local anisotropy and only spin components in this direction order. The correlation length remains finite and substantial magnetization can be induced by small fields. This implies that it is difficult to define a Curie temperature, an observation that has been also made in the case of amorphous Y-Fe alloys.⁷ Magnetic clusters form and decay stochastically with relaxation times increasing with decreasing temperature until at a temperature T_{xy} the perpendicular components also freeze and a noncollinear configuration is established. In this picture the final state would depend on the presence of a magnetic field and has probably a metastable character as shown by the TRM and IRM results. Further studies of the time dependence of the remanent magnetization and relaxation effects in Mössbauer spectra may help to substantiate this picture. Small-angle neutron-scattering (SANS) measurements and further

magnetic measurements on single crystals would be definitive for understanding the nature of the observed MTP.

CONCLUSIONS

A variety of experimental results from ac and dc magnetometry and Mössbauer spectroscopy, summarized in Table II, gives strong evidence that the magnetic state of the intermetallic compounds $\text{YFe}_{10}\text{Mo}_2$ and $\text{LuFe}_{10}\text{Mo}_2$ is established by an initial ferromagnetic-like ordering of components along a preferred direction. The transverse components fluctuate rapidly and freeze with decreasing temperature into a spin-glass-like configuration leading to a noncollinear arrangement of magnetic moments. This state is formed under the combined effect of competition of positive and negative magnetic exchange interactions, the reduced strength of the exchange interactions characteristic of the Mo compounds of this series of alloys, and the randomness introduced by the distribution of the Mo atoms in the i site of the ThMn_{12} type structure. The results can be interpreted in the light of theoretical models which are based on a distribution of exchange interactions extending to negative values of J . In the phase diagram proposed by Ryan *et al.*² the studied alloys would be placed in the borderline between ferromagnetic behavior and a mixed magnetic state, with the Y alloy closer to the ferromagnetic regime as evidenced by the difference in hysteresis behavior and the ordering temperature with regard to the Lu alloy.

As magnetically concentrated systems dominated by direct exchange these alloys provide a useful comparison with other crystalline alloys in which transverse spin freezing is more usually observed close to the percolation threshold² where a crossover from long-range to short-range coupling occurs. The $\text{RFe}_{10}\text{Mo}_2$ alloys consist of a *unique crystalline intermetallic* system, with a well-defined site occupation of the R and Fe-Mo atoms, where the different R^{3+} ions control the more or less ferromagnetic-like behavior. In contrast, for the crystalline solid solution systems $\text{Au}_{100-x}\text{Fe}_x$ ($1 < x < 35$) and $\text{Fe}_{100-x}\text{Al}_x$ ($x \sim 25$), the spin-glass-like properties observed in some members are controlled by the concentration of the magnetic element.

Generally, the iron-rich intermetallic $\text{RFe}_{10}\text{Mo}_2$ compounds provide a very attractive alternative crystalline system for studying the effects of varying exchange frustration on magnetic ordering. However, the present data should be considered preliminary for the correct explanation of the nature of the observed transitions. The possibility of single crystals preparation and their examination with neutrons is a very promising aspect for the exact determination of the magnetic phases reported here.

ACKNOWLEDGMENT

This work was supported in part by the Commission of the European Communities in the framework of the CEAM program.

- ¹K. Moorjani and J. M. D. Coey, *Magnetic Glasses* (Elsevier, New York, 1984).
- ²D. H. Ryan, J. O. Strom-Olsen, R. Provencher, and M. Townsend, *J. Appl. Phys.* **64**, 5787 (1988).
- ³H. Hiroyoshi and K. Fukamishi, *J. Appl. Phys.* **53**, 2226 (1982).
- ⁴N. Saito, H. Hiroyoshi, K. Fukamishi, and Y. Nakagawa, *J. Phys. F* **16**, 911 (1986).
- ⁵J. J. Rhyne and G. E. Fish, *J. Appl. Phys.* **57**, 3407 (1985).
- ⁶M. Ghafari, W. Keune, R. A. Brand, R. K. Day, and J. B. Dunlop, in *Proceedings of the Sixth International Conference on Rapidly Quenched Metals (RQ6)*, edited by R. W. Cochrane and J. O. Strom-Olsen [*Mater. Sci. Eng.* **99**, 65 (1988)].
- ⁷J. M. D. Coey, D. Givord, A. Lienard, and J. P. Rebouillat, *J. Phys. F* **11**, 2707 (1981); J. Chappert, J. M. D. Coey, A. Lienard, and J. D. Rebouillat, *ibid.* **11**, 2727 (1981).
- ⁸M. Gabay and G. Toulouse, *Phys. Rev. Lett.* **47**, 201 (1981).
- ⁹J. M. D. Coey, A. Lienard, J. P. Rebouillat, D. H. Ryan, Y. Boliang, and W. Zhenxi, *J. Phys. F* **18**, 1299 (1988).
- ¹⁰Bo-Ping Hu, Hong-Shuo Li, J. P. Gavigan, and J. M. D. Coey, *J. Phys. Condens. Matter* **1**, 755 (1989).
- ¹¹W. G. Haije, J. Spijkerman, F. F. de Boer, K. Bakker, and K. H. J. Buschow, *J. Less-Common Met.* **162**, 285 (1990).
- ¹²C. Christides, M. Anagnostou, Hong-Shuo Li, A. Kostikas, and D. Niarchos, *Phys. Rev. B* **44**, 2182 (1991).
- ¹³C. Christides, Ph.D. thesis, 1991.
- ¹⁴X. C. Kou, C. Christides, R. Grossinger, H. R. Kirchmayr, and A. Kostikas, *J. Magn. Magn. Mater.* **105-107**, 1341 (1992).
- ¹⁵C. Christides, Hong-Shuo Li, A. Kostikas, and D. Niarchos, *Physica B* **175**, 329 (1991).
- ¹⁶I. Felner and I. Nowik, *J. Magn. Magn. Mater.* **58**, 169 (1986).
- ¹⁷J. Gal, I. Yaar, E. Arbaboff, H. Etedgi, F. J. Litterst, K. Agrawal, J. A. Pereda, G. M. Kalvius, G. Will, and W. Schaffer, *Phys. Rev. B* **40**, 745 (1989).
- ¹⁸V. Psycharis, M. Anagnostou, C. Christides, and D. Niarchos, *J. Appl. Phys.* **70**, 6122 (1991).
- ¹⁹K. H. J. Buschow and D. B. de Mooij, in *Concerted European Action on Magnets (CEAM)*, edited by I. V. Mitchell *et al.* (Elsevier, New York, 1989), p. 63.
- ²⁰H. Wakabayashi, T. Goto, K. Fukamichi, and H. Komatsu, *J. Phys. Condens. Matter* **2**, 417 (1990).
- ²¹G. S. Grest, C. M. Soukoulis, and K. Levin, *J. Appl. Phys.* **55**, 1634 (1984); C. M. Soukoulis, K. Levin, and G. S. Grest, *Phys. Rev. B* **28**, 1495 (1983); **28**, 1510 (1983).
- ²²J. J. Prejean, M. J. Joliclerc, and P. Monod, *J. Phys. (Paris)* **41**, 427 (1980).
- ²³M. Shimizu and H. Kobayashi, *J. Phys. Soc. Jpn.* **53**, 2111 (1984).
- ²⁴L. Néel, *Ann. Phys. (Paris)* **5**, 232 (1936).
- ²⁵W. Kummerle and U. Gradmann, *Solid State Commun.* **24**, 33 (1977).
- ²⁶D. W. Forester, N. C. Koon, J. H. Schelleng, and J. J. Rhyne, *J. Appl. Phys.* **50**, 7336 (1979).
- ²⁷D. Givord and R. Lemaire, *IEEE Trans. Magn. MAG* **10**, 109 (1971).
- ²⁸M. Anagnostou, C. Christides, and D. Niarchos, *Solid State Commun.* **788**, 681 (1991).
- ²⁹A. Posinger, W. Winkler, W. Steiner, A. X. Trautwein, and M. Reissner, *J. Phys. Condens. Matter* **3**, 2713 (1991).